

Cardiac Arteries Disease Finding Using IVUS Images

¹**Remya Gopalakrishnan**, Assistant professor, College of engineering Aranmula, Kerala, India.

²**Priya R Krishnan**, Assistant professor, Cochin University College of engineering kuttanad, Kerala, India.

³**R.Nishanth**, Assistant professor, Cochin University College of engineering kuttanad, Kerala, India.

⁴**Hari Krishnan. D**, Associate professor, Cochin University College of engineering kuttanad, Kerala, India.

⁵**Abin John Joseph**, Assistant professor, Cochin University college of engineering kuttanad, Kerala, India.

⁶**Nidhin Sani**, Assistant professor, Cochin University College of engineering kuttanad, Kerala, India.
remyaharikrishna@gmail.com

ABSTRACT

Intra-Vascular Ultra Sound (IVUS) is a medical imaging technique designed by catheter, which has the miniaturized ultrasound probe, which is attached to the end of the catheter. The computerized ultrasound equipment is attached to the proximal end. The amount of atheromatous plaque built up in the coronary artery is mainly identified by the IVUS image and thus the classification of IVUS images can be used to diagnose coronary artery disease. To enable accurate depiction of atheroma in the walls of coronary artery and progress a detailed perspective and understanding about the classes of the IVUS used for the prediction using mSVM. In this study, a method for Coronary Artery Disease Diagnosis (CADD) system using IVUS is presented. The CADD system uses pre-processing, feature extraction and classification techniques. Firstly, the speckle noise in the different input IVUS images is removed by frost filter. Then Empirical Curvelet Transform (ECT) is used for decomposition. The energy features is used to extract the features from decomposed images. Finally, prediction is made by multiclass Support Vector Machine (mSVM). The system uses different IVUS images (normal, fibro fatty, calcium and thrombus) for performance evaluation. It produces the accuracy of 95 % using ECT based energy features and mSVM.

Keywords: Coronary Artery Diagnosis, Frost Filter, Empirical Curvelet Transform, multiclass Support Vector Machine.

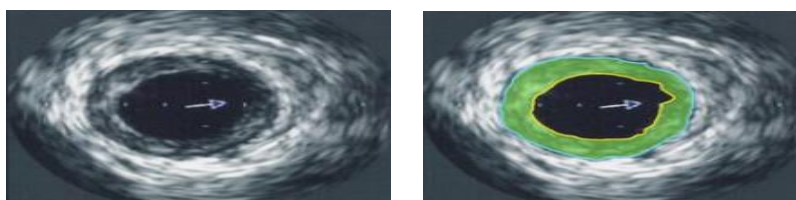
1. INTRODUCTION

IVUS technology is a catheter designed medical imaging technology that is attached to the catheter end by a miniature ultrasound sample. The vessels of people in blood vessels like a piezoelectric transducer can be examined via the ultrasound system. The cardiac arteries (coronal arteries) are the most common target of IVUS imaging. The amount of atheromatous plaster in the coronary artery at any point is determined with coronary artery IVUS. In the wall of the artery and/or artery lumen, IVUS may be helpful to measure all plaque volume.

The most significant use of IVUS is possibly to imagine plaques which angiography is

difficult to see. In clinical research, IVUS therefore made progress to provide a more detailed perspective and a better understanding. Figure 1 shows the IVUS image with coronary plaque.

In figure 1 the IVUS image (a) is a sample IVUS image and (b) denotes the coronary artery with the yellow color coding on the right, the external elastic mucosa is denoted with blue and the green color of the atherosclerotic plaque is denoted. The stenosis in percentage is defined as the yellow area divided by the outside elastic membrane area blue by 100. When plaque burden increases, it will reduce the lumen size and increase the stenosis level.



(a) (b)
Figure 1. (a) IVUS image (b) IVUS image with Coronary artery with plaque

In the early 1990s, studies of IVUS after angioplasty suggested that the re-stenosis issue in the majority was not valid, as shown in an angiography. There appeared to be a sufficiently wider angiographic column, but the newly enlarged lumen contained a considerable plaque which was partially obstructing the lumen. The use of stents to keep the plaque outside the interior walls of the artery out of the lumen was more often encouraged.

Classification of coronary plaque in IVUS images reconstructed is stated in [1]. The stent struts detection is made in the input IVUS images. Then the maximum likelihood regions are determined. Finally, the optimization is made by gentle boost classifiers. Coronary plaque classification using reconstructed IVUS images is discussed in [2]. Initially, the raw reconstructed IVUS image input is given to normalize the image. Then the tissues are automatically classified by texture analysis and adaptive boosting learning technique.

Characterization of plaques using IVUS images is described in [3]. The borders are detected in the input IVUS image, then the features like first order statistical features, gray level co-occurrence matrix, local binary patterns, run-length features and wavelet features are extracted. Then the redundant features are selected by the technique called fuzzy complementary criterion. Then the selected features are classified by Support Vector Machine (SVM) classifier. Blood region in IVUS image classification is discussed in [4] using three dimensional brushlet expansions. Initially, IVUS images are given to brushlet transforms. Then several features of brushlet coefficients are selected by the projections of low frequency brushlet coefficients. The selected coefficients are classified by neural network classifier.

Differentiation and classification of atherosclerotic lesions is presented in [5] using IVUS image and texture features. The IVUS images are given to image acquisition technique.

Then the lesions are segmented and pre-processed, and then the two-dimensional and three-dimensional textures are applied. A principal component analysis is used for feature selection and classifies the lesions. IVUS image modeling is discussed in [6] for statistical strategy in anisotropic adventitia. At first, the input images are preprocessed by using polar coordinates smoothed by restricted anisotropic diffusion technique. Then the statistical selection and border points are extracted by using feature space design. The vessel borders are segmented and vessel structure is classified.

IVUS registration methods are discussed in [7]. The IVUS images are pre-processed by full image region and segmented vessel wall region. The transversal registration is used to find the rigid motion and align the regions between the two pair of frames. Longitudinal registration is also occurs. Finally, the transversal registration is validated. Characterization of different plaque types using IVUS images is discussed in [8]. Gabor filter is used for pre-processing, then modified wavelet transform is used for extraction of features and SVM classifier is used for prediction of output.

Coronary IVUS sequences is discussed in [9] for automatic bifurcation detection. Initially, the image gating and rigid registration is made for artifact compensation. Then the features like parametric texture maps and statistical analysis are extracted. The redundant features are selected. At last, prediction is made by state-of-art discriminative classifiers like random forest, SVM and adaptive boosting. A textural approach for soft and hard plaque detection in IVUS image is described in [10]. Rectangular to polar transformation is applied for input IVUS images. Gray level co-occurrence matrix is used for extracting features. Fuzzy-c means technique is used for segmentation. The region of interest is extracted. A morphological operation is used to

remove the unwanted regions to perform accurate segmentation of plaque.

Detection of media adventitia borders in IVUS images is described in [11] using auto encoder neural network. The mean filter is used for pre-processing and smoothing the IVUS images. Then the artificial neural network is used for prediction of media adventitia borders. Characteristic identification and texture analysis is discussed in [12] using IVUS image plaque tissues. The combination of co-occurrence matrix and fraction methods are used to extract the features. The projective matrix is used to identify the projected vector. Fisher linear discriminant classifier is used for prediction.

IVUS image for despeckling the wavelet based non local means filter is described in [13]. At first, noise is added to image. The wavelet transform is used for decomposition of noisy image and produce the coefficients. The only approximate coefficient is used for further process. Inverse transform is applied for detailed coefficient and

non-local means filter image finally the image is filtered. IVUS classification using non-negative matrix factor and maximum likelihood classifier is described in [14]. The frost filter is applied for pre-processing. Then non matrix factorization technique is used for feature extraction. At last, maximum likelihood classifier is used for classification.

2. PROPOSED RESEARCH WORK

The CADD system consists of 3 important stages they are; (i) Pre-processing, (ii) Feature extraction and (iii) Classification. The detailed workflow of CADD system is shown in figure 2. In first stage, the speckle noise in the different class IVUS image is removed by frost filter pre-processing stage. The noise removed image is decomposed by ECT and produce the sub-band coefficients. These sub-band coefficients are extracted by using energy feature and stored in the database. Finally, the prediction is made by mSVM.

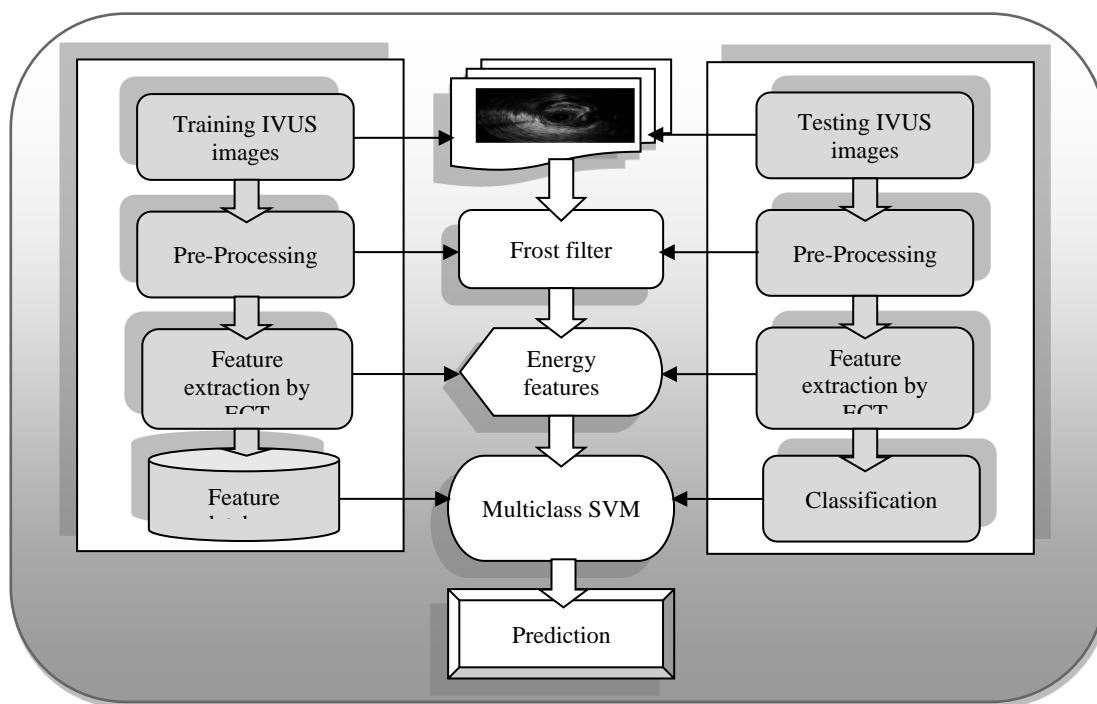


Figure 2. Proposed work

The gel filter works to preserve edges while suppressing the noise on the basis of local statistical data in a sliding window. The Frost filter

is a circularly symmetric filter, exponentially damped, using local statistics. An exponential damping factor is the main factor in regulating the

smoothness of the filter. The picture is normally smooth when the damping factor is low. The frost filter is defined by,

$$K = \frac{\sum(z * Y)}{\sum Y} \tag{1}$$

Where z is the local window pixel values, K is a filtered pixel value in the local window, Y is the weight for local window. The frost filter is also

used in other image processing techniques like adaptive histogram equalization method [15] and adaptive tuning factor and adaptive windowing [16]. In this study, the frost filter is used to remove the speckle noise from the input IVUS images.

The main idea behind the ECT is to create a filter bank on a “polar wedge” in the Fourier region. Figure 3 shows the Fourier plane curvelet tiling. That angle is split into dyadic intervals and repeated on both levels. The dimensions and angles of each polar wedge are measured empirically.

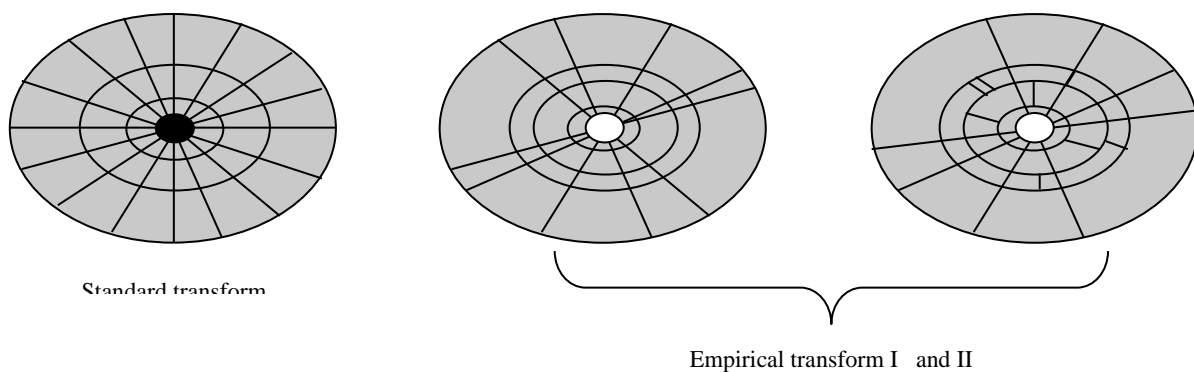


Figure 3.Tiling of Fourier plane

Let us assume, the number of scales is M_s and the number of angular scales is M_θ . The set of scale boundaries is provided with it such as, $\Omega_\nu = \{\nu^n\}_{n=0, \dots, N_s}$ and then the angular boundaries are $\Psi_\theta = \{\theta^k\}_{k=1, \dots, M_\theta}$.

The Littlewood-Paley transform is equivalent to low pass filter. ECT is also used in other fields like signal enhancement [17] and glaucoma fundus image classification [18-19]. In this study ECT used for decomposition of different IVUS images.

Statistical amounts in general; energy is known as the second angular moment which measures uniformity in texture. In this step, you will calculate the sum of the magnitude of the EWT coefficients in each sub-band. The interpretation is,

$$Energy_{E_n} = \frac{1}{OP} \sum_{m=1}^O \sum_{n=1}^P |P_{m,n}^{E_n}| \tag{2}$$

Where O and P are considered to be the sub-band height and width and $P_{m,n}^{E_n}$ is the ECT coefficient of E_n be the sub-band location (m, n) . The energy features are also used in other image processing techniques like human action recognition [20] and weld image classification [21]. The decomposed IVUS images are extracted by using energy features and stored in feature database.

Instances where labels are taken from a finite set of several elements, mSVM aims at allocating labels to SVM. The main solution is to reduce the problem of multiple classes to several binary classification problems. These methods include common methods for reduction includes,

- Create binary classifications that differentiate one label from the other or each pair of classes.
- A winner-to-all strategy is used for classifying new instances for all cases in which classes are assigned by the classifier.

- Error-correcting output codes.
- Directed acyclic graph mSVM.

3. RESULTS

The CADD system performances for IVUS image is described in this section. The IVUS

images used to evaluate the CADD system are obtained from Shifa hospitals, Tirunelveli, Tamilnadu, India. Also, the ground truth data is attained from the experienced cardiologists. Figure 4 shows the some of the sample images in the database.

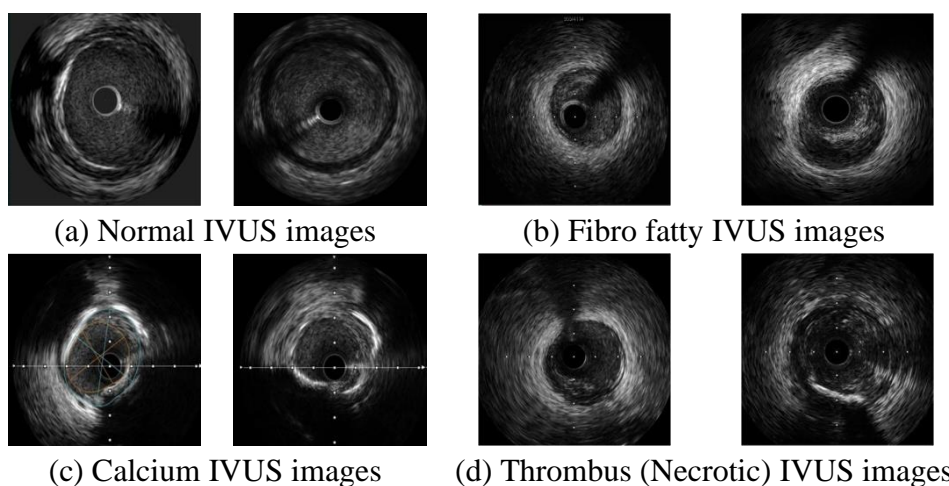


Figure 4. Sample IVUS images in dataset

The CADD system uses ECT based energy features and mSVM for the prediction of IVUS images into four classes of IVUS images like normal (Class-A), calcium (Class-B), fibro fatty (Class-C) and thrombus (Class-D) are used for classification. The input IVUS images are decomposed by ECT up to 4 levels and then energy features is used for feature extraction. Finally, mSVM is used for prediction of different IVUS images into multiclass. The mSVM uses k-fold (10-fold) cross validation technique for prediction of output. Table 1 shows the description about the dataset used in the CADD system.

The performance of CADD system is measured in terms of accuracy, sensitivity and

specificity. To compute these measures, confusion matrix is plotted based on the number of correctly classified images and misclassified images. Table 2 shows the confusion matrix of CADD system using ECT-L1 features and the performance measures computed using the confusion matrix in Table 2 is shown in Table 3. The true positive images are denoted by TP that means that the type of abnormal class is correctly classified and TN represents the true negative images that mean the other classes except abnormal classes are correctly classified. Similarly, FP and FN represent false positive and false negative respectively.

Table 1. Description about the dataset used in the CADD system

Type of IVUS images	No. of images	10-fold setting	
		Training data/fold	Testing data/fold
Normal	60	54	6
Calcium	50	45	5
Fibro-fatty	50	45	5
thrombus	50	45	5

Table 2.Confusion matrix of CADD system using ECT-L1 features

	Class-A	Class-B	Class-C	Class-D
Normal	49	3	4	4
Calcium	4	38	5	3
Fibro-fatty	3	4	38	5
thrombus	4	3	3	40

Table 3.Number of classified images per classes of CADD system using ECT-L1 features

	TP	FP	TN	FN	Accuracy (%)	Sensitivity (%)	Specificity (%)
Normal	49	11	139	11	89.52	81.67	92.67
Calcium	38	10	150	12	89.52	76.00	93.75
Fibro-fatty	38	12	148	12	88.57	76.00	92.50
thrombus	40	12	148	10	89.52	80.00	92.50

The performance of CADD system is analyzed using ECT-L1 features at first. It is evident from Tables 2 to 3 that the successful accuracy of four different classes of IVUS images is approximately equal to 89%. Also, the specificity of the CADD system is around 92% while using ECT-L1 features. The sensitivity of the system is 76% for calcium and Fibro-fatty classes and ~80% for normal and thrombus classes. The level of ECT is increased to 2nd level to extract features and then the extracted features are classified using mSVM classifier. Table 4 shows the confusion matrix of CADD system using ECT-L2 features and the performance measures computed using the confusion matrix in Table 4 is shown in Table 5.

The low accuracy results of CADD system for ECT-L4 features than ECT-L3 are clearly shown in tables 8 and 9. The lack of discriminating power and redundant features reduces the accuracy of CADD system by ~2%. Figure 5 indicates the graphical representation of average performance of CADD system for IVUS image classification.

From the above figure it is clearly observed that the ECT-L3 achieves the higher average accuracy of 95.71% comparing with other levels. The sensitivity and specificity are also 91.33% and 97.14%. The decomposition accuracy is decreased at 4th level so the ECT decomposition is stopped at the 4th level.

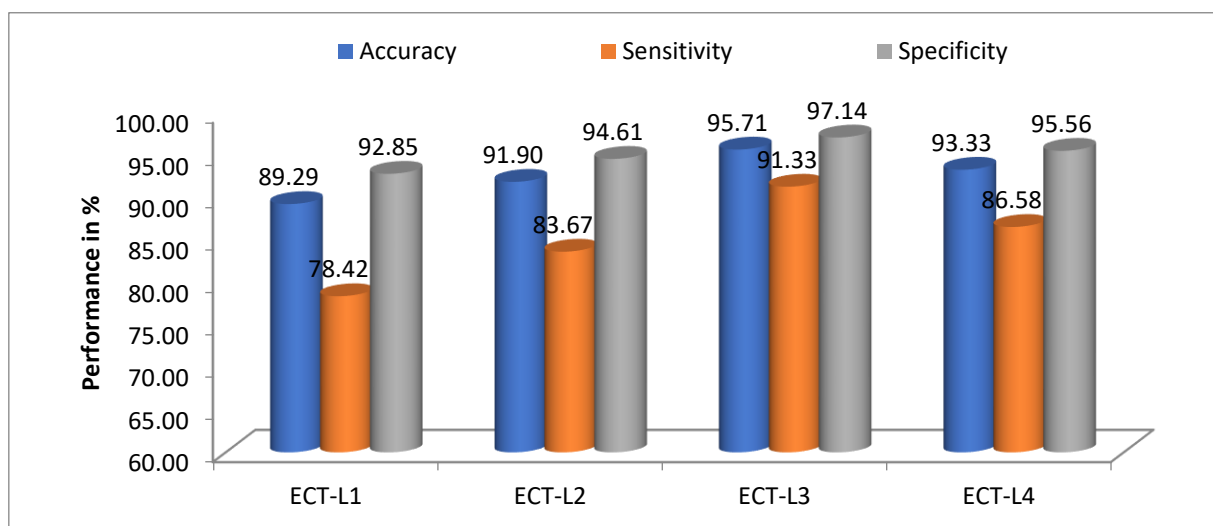


Figure 5. Average performance measure**4. CONCLUSIONS**

A method for CADD system using ECT based energy features and mSVM is presented in this study. The four classes of IVUS images like normal, fibro fatty, calcium and thrombus IVUS images are used for prediction using mSVM. These four classes of images are decomposed by using ECT and sub-band coefficient features are extracted by using energy features and stored in features. The mSVM is used for prediction using *k-fold* cross validation technique. The mSVM predicts the different classes of IVUS images. It achieves the overall accuracy of 95% at the 3rd level of ECT decomposition with 94% sensitivity and 96% specificity by using energy features and mSVM. In future, these techniques may use in different image processing techniques.

REFERENCES

- [1] Rotger D, Radeva P, Bruining N. Automatic detection of bioabsorbable coronary stents in ivus images using a cascade of classifiers. *IEEE Transactions on Information Technology in Biomedicine*. 2009 Mar 16;14(2):535-7.
- [2] Caballero KL, Barajas J, Pujol O, Rodriguez O, Radeva P. Using reconstructed ivus images for coronary plaque classification. In 2007 29th Annual International Conference of the IEEE Engineering in Medicine and Biology Society 2007 Aug 22 (pp. 2167-2170). IEEE.
- [3] Giannoglou VG, Stavrakoudis DG, Theocharis JB. IVUS-based characterization of atherosclerotic plaques using feature selection and SVM classification. In 2012 IEEE 12th International Conference on Bioinformatics & Bioengineering (BIBE) 2012 Nov 11 (pp. 715-720). IEEE.
- [4] Katouzian A, Selver MA, Angelini ED, Sturm B, Laine AF. Classification of blood regions in IVUS images using three dimensional brushlet expansions. In 2009 Annual International Conference of the IEEE Engineering in Medicine and Biology Society 2009 Sep 3 (pp. 471-474). IEEE.
- [5] Brathwaite P, Nagaraj A, Kane B, McPherson DD, Dove EL. Automatic classification and differentiation of atherosclerotic lesions in swine using IVUS and texture features. In *Computers in Cardiology* 2002 Sep 22 (pp. 109-112). IEEE.
- [6] Gil D, Hernández A, Rodríguez O, Mauri J, Radeva P. Statistical strategy for anisotropic adventitia modelling in IVUS. *IEEE Transactions on Medical Imaging*. 2006 May 30;25(6):768-78.
- [7] Talou GD, Blanco PJ, Larrabide I, Bezerra CG, Lemos PA, Feijóo RA. Registration methods for IVUS: transversal and longitudinal transducer motion compensation. *IEEE Transactions on Biomedical Engineering*. 2016 Jun 15;64(4):890-903.
- [8] Roodaki A, Taki A, Setarehdan SK, Navab N. Modified wavelet transform features for characterizing different plaque types in IVUS images; a feasibility study. In 2008 9th International Conference on Signal Processing 2008 Oct 26 (pp. 789-792). IEEE.
- [9] Alberti M, Balocco S, Gatta C, Ciompi F, Pujol O, Silva J, Carrillo X, Radeva P. Automatic bifurcation detection in coronary IVUS sequences. *IEEE transactions on biomedical engineering*. 2012 Jan 3;59(4):1022-31.
- [10] Su S, Gao Z, Zhang H, Lin Q, Hau WK, Li S. Detection of lumen and media-adventitia borders in IVUS images using sparse auto-encoder neural network. In 2017 IEEE 14th International Symposium on Biomedical

- Imaging (ISBI 2017) 2017 Apr 18 (pp. 1120-1124). IEEE.
- [11] Haiyan D, Hong L. Texture analysis and characteristic identification about plaque tissues of IVUS. In 2010 International Conference on Computational and Information Sciences 2010 Dec 17 (pp. 873-876). IEEE.
- [12] China D, Mitra P, Chakraborty C, Mandana KM. Wavelet based non local means filter for despeckling of intravascular ultrasound image. In 2015 International Conference on Advances in Computing, Communications and Informatics (ICACCI) 2015 Aug 10 (pp. 1361-1365). IEEE.
- [13] Rajan, A. (2018). Classification of intravascular ultrasound images based on non-negative matrix factorization features and maximum likelihood classifier. *International journal of advances in signal and image sciences*, 4(1), 16-22.
- [14] Josephus, C. S., & Remya, S. (2011, September). Multilayered contrast limited adaptive histogram equalization using frost filter. In 2011 IEEE Recent Advances in Intelligent Computational Systems (pp. 638-641). IEEE.
- [15] Sun Z, Zhang Z, Chen Y, Liu S, Song Y. Frost Filtering Algorithm of SAR Images With Adaptive Windowing and Adaptive Tuning Factor. *IEEE Geoscience and Remote Sensing Letters*. 2019 Sep 19.
- [16] Dong L, Wang D, Zhang Y, Zhou D. Signal enhancement based on complex curvelet transform and complementary ensemble empirical mode decomposition. *Journal of Applied Geophysics*. 2017 Sep 1;144:144-50.
- [17] Jain S, Sharma SD. Classification of Glaucoma Fundus Images Using Curvelet Empirical Wavelet Transform. In 2019 Fifth International Conference on Image Information Processing (ICIIP) 2019 Nov 15 (pp. 321-325). IEEE.
- [18] Maharaja D, Shaby M. Empirical Wavelet Transform and GLCM Features Based Glaucoma Classification from Fundus Image. *International Journal of MC Square Scientific Research*. 2017 Mar 27;9(1):78-85.
- [19] Xie H, Wu Q. Human action recognition based on variation energy images features. In 2015 11th International Conference on Natural Computation (ICNC) 2015 Aug 15 (pp. 479-484). IEEE.
- [20] Kalaiselvi V, Aravindhar DJ. An Efficient Weld Image Classification System Using Wavelet and Support Vector Machine. In 2019 3rd International Conference on Computing and Communications Technologies (ICCCT) 2019 Feb 21 (pp. 46-49). IEEE.
- [21] XiaoHui W, FengJuan G. Using multiclass svm and mp for audio recognition of action scenes. In 2010 International Conference on Advances in Energy Engineering 2010 Jun 19 (pp. 273-276). IEEE.
- [22] Shanmugan K. GENDER CLASSIFICATION FROM THE IRIS CODE USED FOR RECOGNITION. *International Journal of MC Square Scientific Research*. 2017 Mar 27;9(1):218-29.
- [23] Selamat MH, Rais HM. Image face recognition using Hybrid Multiclass SVM (HM-SVM). In 2015 International Conference on Computer, Control, Informatics and its Applications (IC3INA) 2015 Oct 5 (pp. 159-164). IEEE.
- [24] Mohanan S. Sports video categorization by multiclass svm using higher order spectra features. *International journal of advances in signal and image sciences*. 2017 Dec 28;3(2):27-33.